Revision 1

Uptake and Release of Arsenic and Antimony in Alunite-Jarosite and Beudantite Group Minerals

Karen A. Hudson-Edwards

Environment & Sustainability Institute and Camborne School of Mines, University of Exeter, Penryn, Cornwall TR10 9DF

Submitted to: *American Mineralogist*

Manuscript type: Invited Centennial Review Manuscript

Date of re-submission: 1 February 2019

Keywords: arsenic; antimony; alunite; jarosite; beudantite

This is a preprint, the final version is subject to change, of the American Mineralogist (MSA)
Cite as Authors (Year) Title. American Mineralogist, in press.
DOI: https://doi.org/10.2138/am-2019-6591

ABSTRACT

Arsenic and antimony are highly toxic to humans, animals and plants. Incorporation in alunite, jarosite and beudantite group minerals can immobilize these elements and restrict their bioavailability in acidic, oxidizing environments. This paper reviews research on the magnitude and mechanisms of incorporation of As and Sb in, and release from, alunite, jarosite and beudantite group minerals in mostly abiotic systems. Arsenate-for-sulfate substitution is observed for all three mineral groups, with the magnitude of incorporation being beudantite (3-8.5 wt. % As) > alunite (3.6 wt. % As) > natroalunite (2.8 wt. %) > jarosite (1.6 wt. % As) > natroalunite (1.5 wt. % As) > hydroniumalunite (0.034 wt. % As). Arsenate substitution is limited by the charge differences between sulfate (-2) and arsenate (-3), deficiencies in B-cations in octahedral sites and for hydroniumalunite, difficulty in substituting protonated H_2O-for-OH^- groups. Substitution of arsenate causes increases in the *c*-axis for alunite and natroalunite, and in the *c*- and *a*-axes for jarosite. The degree of uptake is dependent on, but limited by, the AsO_4/TO_4 ratio. Aerobic and abiotic As release from alunite and natroalunite is limited, especially between pH 5 and 8. Release of As is also very limited in As-bearing jarosite, natrojarosite and ammoniumjarosite at pH 8 due to formation of secondary maghemite, goethite, hematite and Fe arsenates that resorb the liberated As. Abiotic reductive dissolution of As-bearing jarosite at pH 4, 5.5 and 7 is likewise restricted by the formation of secondary green rust sulfate, goethite and lepidocrocite that take up the As. Similar processes have been observed for the aerobic dissolution of Pb-As-jarosite (beudantite analogue), with secondary Fe oxyhydroxides resorbing the released As at pH 8. Higher amounts of As are released, however, during microbial-driven jarosite dissolution. Natural jarosite has been found to contain up to 5.9 wt. % Sb^{5+} substituting for Fe^{3+} in the B-site of the mineral structure. Sb(V) is not released from jarosite at pH 4 during abiotic reductive dissolution, but at pH 5.5 and 7, up to 75% of the mobilized Sb can be structurally incorporated into secondary green rust sulfate, lepidocrocite or goethite. Further research is needed on the co-incorporation of As, Sb and other ions

in, and the uptake and release of Sb from, alunite, jarosite and beudantite group minerals, the influence of microbes on these processes and the long-term (>1 year) stability of these minerals.

INTRODUCTION

Arsenic (As) and antimony (Sb) are two of the most toxic elements to humans and many biota (Sundar and Chakravarty 2010; Feng et al. 2013; Abdul et al. 2015). The risks posed by exposure to As and Sb can be mitigated by the precipitation of minerals and especially, those that are relatively insoluble and have low bioaccessibility. Alunite, jarosite and beudantite-group minerals form in oxidizing, low-pH conditions in a wide variety of environments, including mine wastes (Hudson-Edwards et al. 1999; Kocourková et al., 2011; Nieto et al. 2003), acid sulfate soils (Nordstrom 1982; Welch et al. 2007), saline lakes (Alpers et al. 1992) and sulfuric acid caves (D'Angeli et al. 2018). A significant body of work has been carried out to understand the capacity and mechanisms of uptake of As and Sb in, and release from, alunite, jarosite and beudantite-group minerals formed in these environments. The aim of this paper is to synthesize and review research, and to outline research gaps that should be filled by future work.

MINERALS OF THE ALUNITE, JAROSITE AND BEUDANTITE GROUPS

Minerals of the alunite supergroup have a general formula of $AB_3(TO_4)_2(OH)_6$. In the formula, A represents cations with a coordination number greater than or equal to 9, B represents cations in a slightly distorted octahedral coordination, and T represents cations with tetrahedral coordination (Kubisz 1964, 1970; Jambor 1999; Hawthorne et al. 2000; Fig. 1). Within the supergroup, the alunite group minerals contain more Al^{3+} than Fe^{3+}, and jarosite group minerals contain more Fe^{3+} than Al^{3+}, in the B-site (Table 1). The A-site can be filled by univalent or divalent cations such as K^+, Na^+, H_3O^+, Ca^{2+}, Sr^{2+}, Ba^{2+} and Pb^{2+}, but the most common substitutions are K^+ (giving alunite and jarosite), Na^+ (giving natroalunite and natrojarosite) and H_3O^+ (giving hydroniumalunite and hydroniumjarosite). When divalent cations substitute for monovalent cations, charge balance is maintained in the alunite-jarosite structure by creating A-site vacancies with replacement of two monovalent cations by one

66 divalent cation (e.g., plumbojarosite), the incorporation of divalent cations in the B-site (e.g.,
67 beaverite), or the incorporation of trivalent anions in normally divalent anion sites (e.g., beudantite).
68 The T site of alunite supergroup minerals is normally filled by S^{6+} in the sulfate anion SO_4^{2-}, but can
69 also be filled by As^{5+} in AsO_4^{3-}, P^{5+} in PO_4^{3-} and Si^{4+} in SiO_2. The beudandite group contains both
70 SO_4^{2-} and AsO_4^{3-} in the T site, Al^{3+}, Fe^{3+} or Ga^{3+} in the B site, and Ba^{2+}, Pb^{2+} or Sr^{2+} in the B site
71 (Table 1). Solid solutions have been reported to exist between jarosite, plumbojarosite and beudantite
72 (Sànchez et al. 1996).

73 Minerals of the alunite supergroup have $R\bar{3}M$ symmetry, and are formed by (SO_4) tetrahedral -
74 (MO_6) octahedral sheets with $[M_3(OH)_6(SO_4)_2]$ compositions, which are linked by interstitial cations
75 and hydrogen bonds (Hawthorne et al. 2000; Fig. 1). Each of the octahedra are slightly distorted, and
76 have four bridging hydroxyl groups lying in a plane with sulfate oxygens at the apices. Three of the
77 SO_4 tetrahedra are coordinated to Fe octahedra, causing lowering of the SO_4 symmetry from T_d to C_{3v}
78 (Jambor 1999; Becker and Gasharova 2001). The mineral structures often contain A- and B-site
79 vacancies (Dutrizac and Jambor 2000), and 'excess', non-OH water, which is assumed to be in the
80 form of hydronium (H_3O^+) that substitutes for K^+ on the A-site (e.g. Ripmeester et al. 1986; Gale et al.
81 2010).

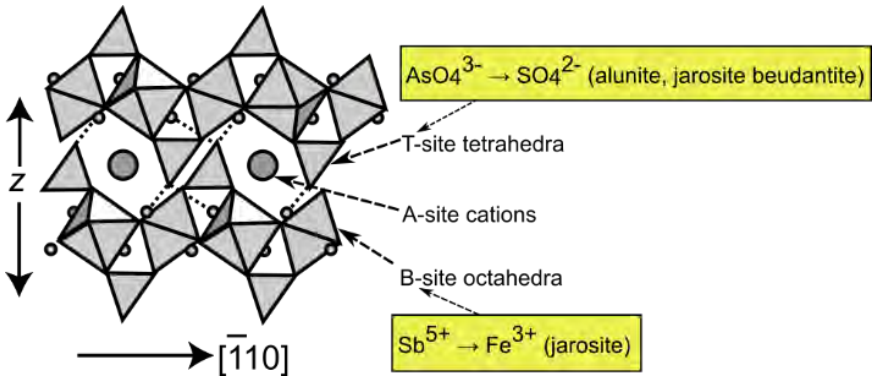

82
83
84 **FIGURE 1**. Structure of minerals of the alunite-jarosite and beudantite groups, showing sites where
85 AsO_4^{3-} and Sb^{5+} substitute in the structure (see text for details).
86
87

This is a preprint, the final version is subject to change, of the American Mineralogist (MSA)
Cite as Authors (Year) Title. American Mineralogist, in press.
DOI: https://doi.org/10.2138/am-2019-6591

TABLE 1. Alunite, jarosite and beudantite family minerals reported to contain As and Sb as major and trace constituents.

Mineral	Formula
Beudantite group minerals with As as a major component	
Beudantite	$PbFe_3(AsO_4)(SO_4)(OH)_6$
Gallobeudantite	$PbGa_3(AsO_4)(SO_4)(OH)_6$
Hidalgoite	$PbAl_3(AsO_4)(SO_4)(OH)_6$
Kemmlitzite	$SrAl_3(AsO_4)(SO_4)(OH)_6$
Alunite-jarosite group minerals with As as a trace component	
Alunite	$KAl_3(SO_4)_2(OH)_6$
Ammoniojarosite	$NH_4Al_3(SO_4)_2(OH)_6$
Natroalunite	$NaAl_3(SO_4)_2(OH)_6$
Hydroniumalunite	$H_3OAl_3(SO_4)_2(OH)_6$
Jarosite	$KFe_3(SO_4)_2(OH)_6$
Natrojarosite	$NaFe_3(SO_4)_2(OH)_6$
Plumbojarosite	$K(Pb,Fe)_3(SO_4)_2(OH)_6$
Jarosite and Beudantite group minerals with Sb as a trace component	
Jarosite	$KFe_3(SO_4)_2(OH)_6$
Beudantite	$PbFe_3(AsO_4)(SO_4)(OH)_6$

UPTAKE OF ARSENIC IN ALUNITE-JAROSITE AND BEUDANTITE GROUP MINERALS

Alunite minerals

To the author's knowledge, no papers have reported the occurrence of natural arsenical members of the alunite family. Arsenate-for-substitution in alunite, natroalunite and hydroniumalunite has been investigated experimentally (Sunyer and Viñals 2011a, b; Sunyer et al. 2013; Luo et al. 2015). Hydroniumalunite takes only up 1 mole % (AsO_4/SO_4+AsO_4) (0.034 wt. % As), possibly due to the difficulty in substituting protonated H_2O-for-OH^- groups in the structure due to blocking by H-bridges of the H_3O (Sunyer et al. 2013). Arsenate substitution is much higher in alunite and natroalunite (up to 3.61 and 2.80 wt. % As, respectively) formed at pH 1 and 2.8-2.9, respectively, and 200 °C (Sunyer et al. 2013; Sunyer and Viñals 2011a). Luo et al. (2015) obtained a slightly lower maximum incorporation of arsenate in natroalunite, giving an approximate molar ratio of 11 (AsO_4/SO_4+AsO_4) % at pH 3.00 and 200 °C.

The degree of uptake of As in alunite and natroalunite is directly related to the AsO_4/TO_4 ratio of the initial solution. Arsenical natroalunite precipitation is favoured at $(AsO_4/TO_4)_{aq} < 0.2$ at 200 °C. At higher $(AsO_4/TO_4)_{aq}$, other arsenate phases such as alarsite ($AlAsO_4$), mansfieldite ($AlAsO_4 \cdot 2H_2O$) and natropharmacoalumite ($NaAl_4(OH)_4(AsO_4)_3.4H_2O$) form (Sunyer and Viñals 2011a). At 200 °C, the ratio of (AsO_4/TO_4) in the precipitated natroalunite was roughly equivalent to $0.5(AsO_4/TO_4)_{aq}$. Precipitation rates also increased with increasing temperature and AsO_4^{3-} concentrations. Experiments in which gypsum was introduced at the outset resulted in an (Ca/Ca+Na) molar ratio of 4-6% Ca-for-Na substitution and arsenate-for-sulfate substitution.

The degree of arsenate uptake in alunite was also dependent on $(AsO_4/TO_4)_{aq}$, with the degree of substitution increasing as $0.5(AsO_4/TO_4)_{alunite} \sim= 0.5(AsO_4/TO_4)_{aq}$ (Sunyer et al. 2013). Arsenical alunite was the only phase to precipitate at $(AsO_4/TO_4)_{aq} < 0.26$ at 200 °C; above this ratio mansfieldite co-precipitated.

Viñals et al. (2010) precipitated a complex natroalunite ($\sim(Na,Ca)(Al,Fe)_3((S,As,P)O_4)_2(OH)_6$ at $(Al/As)_{aq} = 4.5$) by reacting H_2SO_4-leached and ozoned calcium arsenate wastes produced from copper smelting at 180-200 °C with sodium and aluminum sulfate reagents. At pH 2.8-2.9, the As substitution in the tetrahedral site was 7-8 mole % (AsO_4/SO_4+AsO_4). The degree of substitution increased to a maximum molar ratio of 14% with decreasing $(Al/As)_{aq}$, but mansfieldite also precipitated. Prior gypsum removal and As concentrations of 3.5-7.0 g/L were shown to not affect As incorporation or the nature of the As-bearing phases formed.

The effect of arsenate substitution on the alunite and natroalunite unit cell was investigated by Rietveld refinement. Sunyer and Viñals (2011b) showed that the *c*-parameter slightly increased with arsenate for sulfate substitution due to differences between As-O and S-O distances in the tetrahedral site. In contrast, the *a*-parameter was unaffected by arsenate incorporation. The same findings for alunite were reported by Sunyer et al. (2013).

Jarosite minerals

Naturally-occurring arsenian jarosite has been observed in mine wastes (Acero et al., 2006; Hudson-Edwards et al. 1999, 2005; Kocourková et al., 2011; Savage et al. 2000; Filippi et al. 2015), with concentrations of As up to 2000 pm reported (Savage et al., 2000). Most insights into As incorporation mechanisms into jarosite, however, have been studied experimentally (Paktunc and Jambor 2003; Savage et al. 2005; Karimian et al. 2017). This work has consistently shown that AsO_4^{3-} occupies tetrahedral SO_4^{2-} sites within the jarosite structure. X-ray diffraction and XANES analysis have shown that at least 9.9 wt. % AsO_4^{3-} (1.6 wt. % As) can be structurally incorporated into synthetic jarosite (Paktunc and Dutrizac 2003), with others demonstrating that up to 30% replacement of SO_4^{2-} by AsO_4^{3-} can occur (Savage et al. 2005; Paktunc et al. 2003; Kendall et al. 2013). The limiting factors are proposed to be charge imbalances between sulfate and arsenate, and deficiencies of Fe in octahedral sites (Savage et al., 2005). EXAFS data modelling suggests As-O interatomic distances of 1.68 Å and coordination numbers of 4.6+/- 1.7 to 5.4+/-1.7, confirming the tetrahedral arrangement of O atoms around central As atoms (Paktunc and Dutrizac, 2003). Incorporation of arsenate for sulfate causes little change in the *a*-axis, but lengthening of the *c*-axisup to 0.174 Å (Paktunc and Dutrizac 2003; Savage et al. 2005). Jarosite morphology also becomes more anhedral with increasing incorporation of As (Savage et al. 2005).

Co-incorporation of Pb^{2+} results in a larger proportion of As^{5+} being incorporated in the jarosite structure (33% of the tetrahedral sites) compared to when Pb^{2+} is not incorporated (21%; Aguilar-Carrillo et al. 2018). This was proposed to be due to changes in unit cell dimensions to balance the distortion caused by the substitution of arsenate for sulfate in jarosite. The concentrations of As and Pb in the initial experimental solutions limited As and Pb incorporation. At As/Pb < 1, Pb-As jarosites

(beudantite analogues) formed, but at As/Pb > 1, anglesite and poorly crystalline ferric arsenate phases formed along with the As-Pb jarosite.

Pure synthetic natrojarosites have been shown to have very low amounts of arsenate for sulfate substitution (1.5 wt. %; Dutrizac and Jambor 1987). By contrast, synthetic ammoniumjarosite has been shown to take up to 4.1 wt. % arsenate at a pH of 1.2-1.8 (Flores et al. 2016). The mineral, with a formula of $(NH_4)Fe_{2.45}[(SO_4)_{1.80}(AsO_4)_{0.20}][(OH)_{4.15}(H_20)_{1.85}]$, was shown to remain in residual solids above 700 °C.

Using extended X-ray absorption fine structure (EXAFS) analysis, Gräfe et al. (2008) showed that As^{5+} sorbed to the jarosite surface by forming bidentate-binuclear surface complexes, as it did with goethite. The edge-sharing coordination number was larger for jarosite than for goethite (0.9 Fe atoms at 2.87 Å and 0.3 Fe neighbours at 2.87 Å, respectively). By contrast, the radial distance to the next nearest Fe atom was lower in jarosite (3.22 Å) than in goethite (3.28 Å). These results were attributed to the replacement of SO_4 tetrahedra by AsO_4 tetrahedra. In the presence of Cu^{2+}, As^{5+} was shown to be coordinated by multiple Cu atoms over multiple radial distances, which was modelled to be due to the formation of a euchroite-like $[Cu_2(AsO_4)(OH)\cdot 3H_2O]$ complex on the jarosite surface.

Several studies have considered the role of microbes in the formation of arsenical jarosite. Egal et al. (2009), for example, demonstrated that As-bearing jarosite formed in both biotic and abiotic experiments, suggesting that bacterial iron oxidation was not involved in the process. However, aging and of As-rich schwertmannite produced by microbial oxidation of Fe^{2+} in sulfate solutions yielded As-bearing jarosite at lower pH values, and this might be considered to be indirectly biotically-formed. The jarosite does not take up the As^{3+} released by the schwertmannite.

Beudantite minerals

Most of the research on arsenic incorporation in beudantite group minerals (Table 1) has been done on beudantite itself. Beudantite has been shown to host significant amounts (3-8.5 wt. %) of As in supergene zones (Szymanski, 1988), oxidized massive sulfides and related mine wastes (Foster et al. 1998; Roca et al. 1999; Nieto et al. 2003; Roussel et al. 2000; Gieré et al., 2003; Courtin-Nomade et al. 2016) and metallurgical products (Bigham and Nordstrom 2000). Thus, it has been suggested to immobilize these elements and limit their uptake by plants (e.g., Zheng et al. 2003). In high-sulfide waste at the Berikul Au mine, Kemerovo region, Russia, for example, jarosite-beudantite solid solution minerals have been reported to contain up to 8.5 wt. % As (Gieré et al. 2003). A beudantite from the Tsumeb deposit, Namibia (Natural History Museum collection, London, UK, number BM.1987), containing between 3.4 and 6.4 wt. % As, exhibits zoning in As and S, with molar proportions of these elements exactly mirroring each other (r=-1.0; Fig. 2).

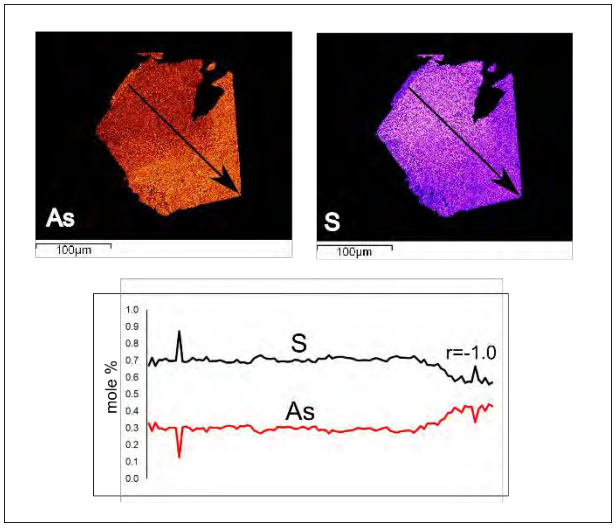

FIGURE 2. Electron microprobe X-ray chemical maps showing zoning of As and S. Black arrow indicates position of line scan of analytical points, for which data are shown in the X-Y plot. Data from K. Hudson-Edwards for sample number BM.1987 from the collections of the Natural History Museum, London, UK. The sample was collected from the 36th level, west 12, of the Tsumeb mine, Grootfontein, Nambia.

196 Other beudantite-group minerals have also been shown to contain significant amounts of As. A
197 sample of hidalgoite from the Tsumeb mine, Namibia, was shown to contain between 7.4 and 10.0 wt.
198 % As (Cooper and Hawthorne 2012). Arsenic-rich kemmlitzite with a T-site formula of
199 $[(AsO_4)_{0.98}(PO_4)_{0.42}(SO_4)_{0.39}(SiO_4)_{0.18}]$ has also been analysed (Jambor 1999). Similarly high amounts
200 of As were found in gallobeudantite from Tsumeb, Namibia, with a formula of
201 $Pb_{1.04}(Ga_{1.39}Fe_{0.82}Al_{0.62}Zn_{0.10})_{3.03}[(AsO_4)_{1.14})(SO_4)_{0.86}]_{2.00}(OH)_{5.94}$ (Jambor et al. 1996).
202 Symanski (1988) showed that the T-site in beudantite, which was filled by arsenate and sulfate,
203 was disordered, and suggested this was due to that the excess negative charge in arsenate compared to
204 sulfate. He further proposed that this disorder was balanced by substitution of hydronium for Pb or by
205 protonation of hydroxyl groups to water.
206 Forray et al. (2014) derived thermochemical data ($\Delta H°_f$ = -3691.2 ± 8.6 kJ/mol; $\Delta G°_f$ = -
207 3164.78 ± 9.1 kJ/mol) and a log K_{sp} value of -13.94 ± 13.94 for the Pb-As jarosite synthesized by
208 Smith et al. (2006). The Pb-As-jarosite had a structure matching that of beudantite (XRD file PDF 19-
209 0689), and composition of $(H_3O)_{0.68}Pb_{0.32}Fe_{2.86}(SO_4)_{1.69}(AsO_4)_{0.31}(OH)_{5.59}(H_2O)_{0.41}$; thus, it did not
210 contain enough Pb or As to be considered true beudantite) The data were used to show that the
211 formation of Pb-As jarosite can decrease aqueous As and Pb concentrations to meet WHO drinking
212 water standards of 10 µg/L (WHO, 1996, 1998; Fig. 3).

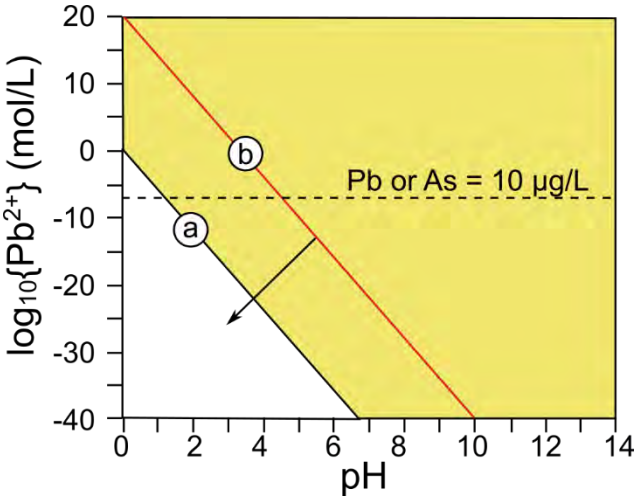

213

FIGURE 3. Stability of Pb–As jarosite as function of pH and lead activity. Point (a) shows the stability boundary for Pb-As jarosite at $a(Fe^{3+}) = 322 \times 10^{-3}$ mol/L, $a(As^{5+}) = 1.33 \times 10^{-7}$ mol/L and $a(SO_4^{2-}) = 1.56 \times 10^{-2}$ mol/L. Point (b) shows the stability boundary for Pb-As jarosite at very low Fe, SO_4 and As activity (10 µg/L each). Reprinted (adapted) from Geochimica et Cosmochimica Acta, 127, Forray et al., Synthesis, characterization and thermochemistry of Pb-As-, Pb-Cu- and Pb-Zn-jarosite compounds, 107-119, Copyright (2014), with permission from Elsevier.

RELEASE OF ARSENIC FROM ALUNITE-JAROSITE AND BEUDANTITE GROUP MINERALS

Alunite minerals

The suitability of alunite, natroalunite and hydronium alunite as short- and long-term stable stores of arsenic has been explored by Viñals et al. (2010), Sunyer and Viñals (2011a, b), Sunyer et al. (2013) and Luo et al. (2015). Sunyer et al. (2013) and Sunyer and Viñals (2011b) showed that after 24 h, arsenical alunite and natroalunite, respectively, released only 0.01-0.05 mg/L As between pH 5 and 8. (Fig. 4). Within 2.5 weeks, arsenical alunite dissolved to release 0.3 mg/L As between pH 4 and 5 (Sunyer et al. 2013). Longer-term stability tests carried out over 6 months by Viñals et al. (2010) showed that natroalunite only released 0.01 mg/L As between pH 4 and 5. These As releases are similar to, or lower than those of natural scorodite ($FeAsO_4.2H_2O$; 0.4 mg/L As) and synthetic scorodite (1.3 mg/L As) (Sunyer and Viñals 2011b). Thus, both arsenical alunite and especially, natroalunite, could be considered as good long-term stores of As-bearing wastes with large SO_4^{2-}/AsO_4^{3-} ratios.

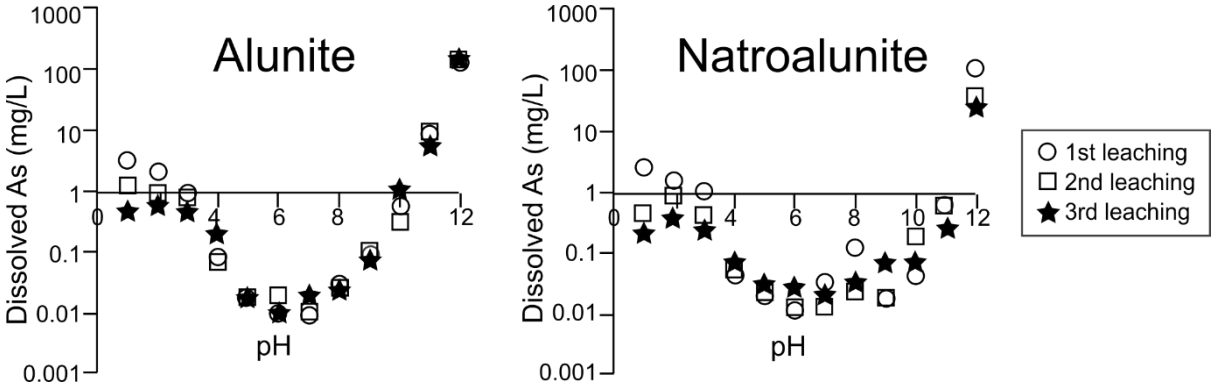

FIGURE 4. Dissolved As (mg/L) as a function of pH for alunite and natroalunite 24 h dissolution experiments. Reprinted (adapted) from Arsenic immobilization as alunite-type phases: The arsenate substitution in alunite and hydronium alunite. Journal of Hazardous Materials, 261, Sunyer et al., 559-569 Copyright (2013) with permission from Elsevier, and Arsenate substitution in natroalunite: A potential medium for arsenic immobilization. Part 2: Cell parameters and stability tests. Hydrometallurgy 109, Sunyer and Viñals, J., 106-115, Copyright (2011) with permission from Elsevier.

The dissolution of arsenical natroalunite has been shown to be congruent at pH 3 and pH 12, and incongruent at pH between 4 and 11 (Sunyer and Viñals 2011b). The mechanism proposed for the incongruent dissolution involves the formation of secondary Al hydroxides, as follows:

$$NaAl_3(SO_4)_{2-x}(OH)_{6-x(s)} + (3+x)H_2O_{(l)} \rightarrow Na^+_{(aq)} + (2-x)SO_4^{2-}{}_{(aq)} + xAsO_4^{3-}{}_{(aq)} + 3Al(OH)_{3(s)} + (3+x)H^+_{(aq)}$$

Jarosite minerals

Kendall et al. (2013) investigated the dissolution of arsenojaroites in pH 2 and 8 solutions and in ultrapure water. Unlike jarosite, the dissolution of arsenojarosite was not pH-dependent. This was proposed to be due to the presence of surface arsenate-iron complexes that prevented protonation at low pH and hydroxyls at high pH. Arseniojarosite dissolution was incongruent, with maghemite, goethite and hematite forming in ultra-pure water experiments, and ferrihydrite in pH 8 Tris-buffered experiments. Short-term dissolution rates were observed to increase with increasing incorporation of arsenate. These rates were attributed to polarization of bonds within the jarosite structure due to

substitution of arsenate, which is larger and higher charged than sulfate. This process would make these bonds more susceptible to dissolution. Preferential leaching of K^+ and SO_4^{2-} compared to Fe^{3+} (cf., Smith et al. 2006) causes enrichment of arsenate-iron complex sites on the surface. Dissolution is then inhibited due to the fact that arsenate-iron complexes are more strongly bonded than sulfate-iron complexes within the structure.

The alkaline decomposition of As-bearing jarosite minerals results in the formation of secondary Fe hydroxides that take up the released As. For example, Patiño et al. (2013) showed that the reaction of a synthetic sodium arsenojarosite ($Na_{0.87}(H_3O)_{0.13}]Fe_{2.50}[(SO_4)_{1.95}(AsO_4)_{0.05}][(OH)_{4.45}(H_2O)_{1.55}]$) with CaOH and NaOH at pH 12.33-12.87 caused an $Fe(OH)_3$ with adsorbed AsO_4 coating to form on the original reactant. The decomposition of arsenic-bearing ammoniumjarosite using NaOH at pH 12.90 and 30°C also resulted in the formation of a secondary Fe arsenate with a composition of 2.45 $Fe(OH)_3 \cdot 0.20\ AsO_4^{3-}$ (Flores et al., 2016).

Karimian et al. (2017) determined the mechanisms and magnitude of As release during the reductive dissolution of jarosite by Fe^{2+} at pH 4.0, 5.5 and 7. At pH 4, the jarosite did not change or release As^{5+} (Fig. 5). At pH 5.5, the jarosite transformed first to green rust (after 60 min) and then to goethite (after 24th), and the As released was taken up on the jarosite surface mostly by labile (c. 10%) and poorly crystalline Fe^{3+}-associated phases (10-30 %). At pH 7, the jarosite transformed rapidly (<10 min) to green rust and then to goethite at high Fe^{2+} concentrations (10 and 20 mM), and to lepidocrocite (< 60 min) at low Fe^{2+} concentrations (1 and 5 mM) (Fig. 5). Some of the original As^{5+} in the jarosite was reduced to As^{3+} in the high Fe^{2+} experiments but not in the low Fe^{2+} experiments. As in the pH 5.5 experiments, the low concentrations of $As_{(aq)}$ suggested that the As released during dissolution was taken up by the secondary Fe^{3+} phases either by surface sorption or incorporation in structural defects.

This is a preprint, the final version is subject to change, of the American Mineralogist (MSA)
Cite as Authors (Year) Title. American Mineralogist, in press.
DOI: https://doi.org/10.2138/am-2019-6591

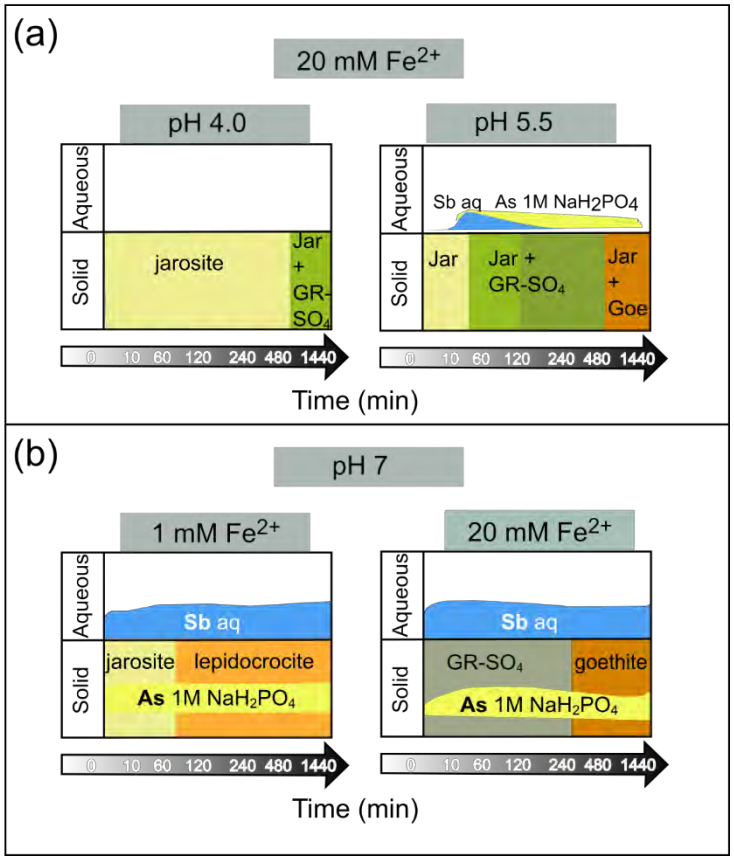

FIGURE 5. Schematic diagram showing results of reductive dissolution of As- and Sb-bearing jarosite by Fe^{2+} at pH 4, 5.5 and 7. See text for discussion. (a) Reprinted (adapted) from Antimony and arsenic partitioning during Fe^{2+}-induced transformation of jarosite under acidic conditions Chemosphere, 195, Karimian et al., 515-523, Copyright (2018) with permission from Elsevier. (b) Adapted with permission from Karimian et al. (2017). Copyright 2017 American Chemical Society.

Sulfide-promoted reductive dissolution of As^{5+}-bearing jarosite resulted in its replacement by mackinawite and mobilization of the As (Johnson et al., 2012). Increasing S^{2-}:Fe ratios and decreasing pH resulted in increased As mobility, except at high S^{2-}:Fe and pH 4.0 when an orpiment-like phase (detected using transmission electron microscopy, TEM) formed. EXAFS analysis was used to show the transition from O-coordinated As^{5+} to S-co-ordinated As^{-} in the orpiment phase.

T

Beudantite minerals

Batch dissolution experiments using a synthetic Pb-As-jarosite (beudantite analogue, see above) were conducted at 20 °C and pH 2 and 8, to mimic environments affected by acid rock/acid mine

drainage, and those remediated with slaked lime ($Ca(OH)_2$), respectively (Smith et al. 2006). The dissolutions were both incongruent. Dissolution at pH 2 yielded poorly crystalline solid $PbSO_4$ (Fig. 6) and aqueous Fe, SO_4^{2-} and AsO_4^{3-}. Dissolution at pH 8, by contrast, produced $Fe(OH)_3$ that resorbed aqueous AsO_4^{3-} and solid $PbSO_4$.

These results were explained by the preferential dissolution of the A- and T-sites, containing Pb and SO_4^{2-} - AsO_4^{3-}, respectively, relative to the sterically remote and Fe octahedra within the T-O-T Pb-As-jarosite structure. By contrast, Roca et al. (1999) suggested that the alkaline decomposition of beudantite in $Ca(OH)_2$ was very slow between 80 and 100 °C. They proposed a slightly different mechanism for beudantite decomposition than Smith et al. (2006), involving the reacton of the beudantite with OH- and water, and production of $Fe(OH)_3$, $Pb(OH)_2$, an As_2O_5 gel and sulfate ions.

Few studies have investigated the role of microbial processes on As- or Sb- bearing alunite-group minerals. One example is that of Smeaton et al. (2012), who used the Pb-As-jarosite phase synthesized by Smith et al. (2006) to conduct reductive dissolution experiments using *Shewanella putrefaciens* at circumneutral pH. The experiments resulted in immediate Fe^{3+} reduction and As^{5+} reduction within 72 h. After 336 h, 20.2% and 3.0% of the total As occurred as solid and aqueous As^{3+}. At this time, secondary Fe-O precipitates containing minor As and Pb formed, leaving c. 0.05 mM As^{3+} and 2 mM As^{5+} in solution. Based on these results, the authors suggested that Pb-As-jarosite would not be a good candidate for long-term As storage under reductive conditions. The reduction of Fe^{3+} was proposed to be thermodynamically driven, while that of aqueous As^{5+} was proposed to be due to microbial detoxification.

This is a preprint, the final version is subject to change, of the American Mineralogist (MSA)
Cite as Authors (Year) Title. American Mineralogist, in press.
DOI: https://doi.org/10.2138/am-2019-6591

(a) 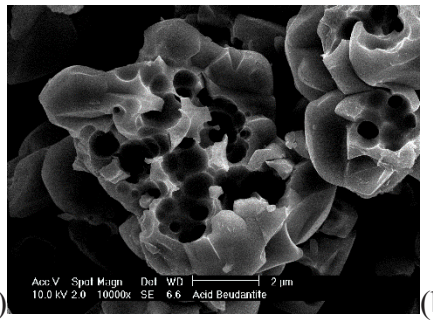

(b) 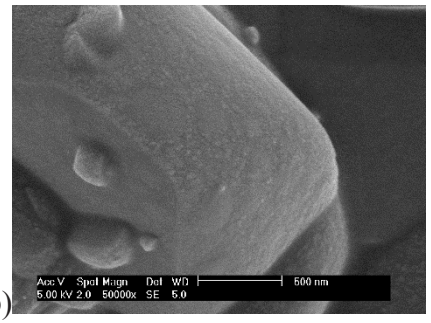

FIGURE 6. Scanning electron microscope (SEM) image of residual solids from the pH 2 dissolution of Pb-As-jarosite, showing (a) extensive pitting of the surface and (b) poorly crystalline secondary $PbSO_4$ on the mineral surface. Reprinted (adapted) from Chemical Geology, 229, Smith et al., Dissolution of lead- and lead-arsenic jarosites at pH 2 and 8: insights from batch experiments, 344-361, Copyright (2006), with permission from Elsevier.

UPTAKE AND RELEASE OF ANTIMONY IN JAROSITE GROUP MINERALS

The mechanisms and magnitudes of incorporation and release of Sb from alunite, jarosite or beudantite family minerals have received much less attention than those of As. The few studies available have focused on the uptake of Sb in, and release of Sb from, jarosite; none, to the author's knowledge, have determined whether alunite or beudantite minerals can take up and release Sb.

Jamieson et al. (2005) reported minor uptake of Sb in jarosite (176 ± 159 ppm, n= 18) forming from waste waters of the Richmond Mine, Iron Mountain, California. By contrast, Courtin-Nomade et al. (2012) found very high concentrations of Sb (59000 ± 21000 ppm) in secondary cryptocrystalline jarosite in historic mill tailings from the French Massif Central. They attributed this to substitution of Sb^{5+} for Fe^{3+} in the jarosite structure, analogous to that occurring in dussertite ($Ba(FeSb)_3(AsO_4)(OH,H_2O)_6$; Kolitsch et al. 1999). Karimian et al. (2017) synthesized an Fe-deficient jarosite (K:Fe:S = 1:2.5:1.9, compared to 1:3:2 for ideal jarosite) that incorporated 1.43 ppm Sb^{5+}. They also proposed that Sb^{5+} substituted for Fe^{3+} in the jarosite structure due to similar ionic sizes (Sb^{5+}, 0.60 Å; Fe^{3+} 0.65 Å) and similar bond lengths in the Sb_VO_6 and $Fe_{III}O_6$ octahedra (Sb-O, 1.91 Å; Fe-O, 1.97-2 Å; Mitsunobu et al. 2013). Such Sb^{5+} substitution for Fe^{3+} has been observed for other Fe^{3+}

346 oxides such as ferrihydrite and goethite (Leuz et al. 2006; Mitsunobu et al. 2010). Courtin-Nomade et
347 al. (2012) reported low concentrations of Sb in streams draining the mine waste dumps, and suggested
348 that this was due to the insolubility of this jarosite under the prevailing conditions (circum-neutral pH)
349 or to the formation of secondary Sb-bearing products from the dissolution of the Sb-bearing jarosite.
350 The reductive dissolution of Sb^{5+}-bearing jarosite by Fe^{2+} under acidic pH (4.0 and 5.5) and
351 neutral pH (7) conditions has been examined (Karimian et al. 2018). No transformation of the jarosite,
352 nor release of Sb^{5+} was observed at pH 4.0 (Fig. 5). This was attributed to the surface of jarosite being
353 positively charged at pH 4.0, thus decreasing the possibility of Fe^{2+} to sorb, and hindering electron
354 transfer and dissolution. In contrast, at pH 5.5, the jarosite transformed to metastable green rust sulfate
355 within c. 60 min. and then to goethite within 24 h (Fig. 5). The pH used in these experiments was very
356 close to point of zero charge (5.6; Xu et al., 2013), and therefore the jarosite surface is near-neutrally
357 charged, allowing greater interaction of Fe^{2+} with the surface and formation of the green rust sulfate
358 and goethite. In these experiments, almost all of the released Sb^{5+} was structurally incorporated within
359 these secondary phases. At pH 7, the Sb was rapidly mobilized into the aqueous phase as Sb^{5+}, but 75%
360 of this Sb^{5+} was structurally incorporated into secondary lepidocrocite (at Fe^{2+} = 1 mM), green rust and
361 goethite (at Fe^{2+} = 20 mM) (Fig. 5).
362
363 **IMPLICATIONS**
364 The incorporation of As in alunite, jarosite and beudantite group minerals (by replacement of
365 SO_4^{2-} by AsO_4^{3-} in the T-site of the mineral structure), and of Sb in jarosite group minerals (by
366 replacement of Fe^{3+} by Sb^{5+} in the B-site; Fig. 1) has important implications for storage of these
367 metalloid contaminants in acidic environments. Since incorporation of Pb^{2+} in the jarosite structure has
368 been shown to cause a higher degree of As take up than with no Pb^{2+} (Aguilar-Carrillo et al. 2018),
369 further research should be carried out to evaluate the effectiveness of this and other ions for

incorporation of greater amounts of As and Sb in alunite, jarosite and beudantite group minerals. Overall, there is a paucity of information on the uptake of Sb in these minerals, despite the fact that it has been shown to be incorporated in jarosite, and that As and Sb are often co-located in contaminated environments (e.g., Craw et al. 2004). This research gap needs to be filled, as does further work on the longer term (>1 year) stability, and abiotic and, especially, microbial dissolution, of As- and Sb-bearing alunite, jarosite and beudantite group minerals.

ACKNOWLEDGEMENTS

I would like to sincerely thank colleagues with whom I have worked with, and had discussions about, arsenic, antimony and minerals of the alunite supergroup. There are many of you but I would like to especially thank Pat Acero, Bill Dubbin, Dave Craw, Ference Forray, Julian Gale, Heather Jamieson, David Kossoff, Peter Cogram, Pam Murphy, Christina Smeaton, Adrian Smith, Mark Welch and Kate Wright. Bill Dubbin provided the beudantite sample BM.1987, and Andy Beard assisted with the electron microprobe chemical mapping. My own work on these minerals has been supported by grants from the UK Natural Environment Research Council (GR9/04094), the UK Engineering and Physical Sciences Research Council (PhD studentship to Adrian Smith), the European Union (IEF 327194), the Royal Society and synchrotron beamtime from CCLRC Daresbury Laboratory (46-068 and 39-310). The manuscript was improved by comments from an anonymous reviewer and associate editor Andrew Elwood Madden.

REFERENCES

Abdul, K.S.M., Jayasinghe, S.S., Chandana, E.P.S., Jayasumana, C., De Silva, P.M.C.S. (2015) Arsenic and human health effects: A review. Environmental Toxicology and Pharmacology, 40, 828-846.

Acero, P., Ayora, C., Torrentó, C., and Nieto, J.-M. (2006) The behavior of trace elements during schwertmannite precipitation and subsequent transformation into goethite and jarosite. Geochimica et Cosmochimica Acta, 70, 4130-4139.

Aguilar-Carrillo, J., Villalobos, M., Pi-Puig, T., Escobar-Quiroz, I.N., and Romero, F.M. (2018) Synergistic arsenic(V) and lead(II) retention on synthetic jarosite. I. Simultaneous structural incorporation behaviour and mechanism. Environmental Science: Processes & Impacts, 20, 354-369.

Alpers, C.N., Rye, R.O., Nordstrom, D.K., White, L.D., and King, B. (1992) Chemical, crystallographic and stable isotopic properties of alunite and jarosite from acid-hypersaline Australian lakes. Chemical Geology, 96, 203-226.

Becker U., and Gasharova B. (2001) AFM observations and simulations of jarosite growth at the molecular scale: probing the basis for incorporation of foreign ions into jarosite as a storage mineral. Physics and Chemistry of Minerals, 28, 545–556.

Bigham, J.M., and Nordstrom, D.K. (2000) Iron and aluminium hydroxysulfates from acid sulfate waters. In Alpers, C.N., Jambor, J.L. & Nordstrom, D.K. (eds.) Sulfate Minerals. Crystallography, Geochemistry and Environmental Significance. Reviews in Mineralogy and Geochemistry, 40, pp. 351-403.

Cooper, M.A., and Hawthorne, F.C. (2012) Refinement of the crystal structure of zoned philipsbornite-hidalgoite from the Tsumeb mine, Namibia, and hydrogen bonding in the $D^{2+}G_3^{3+}(T^{5+}O_4)(TO_3OH)(OH)_6$ alunite structures. Mineralogical Magazine, 76, 839-849.

Courtin-Nomade, A., Rakotoarisoa, O., Bril, H., Brybos, M., Forestier, L., Foucher, F., and Kunz, M. (2012) Weathering of Sb-rich mining and smelting residues: Insight in solid speciation and soil bacteria toxicity. Chemie der Erde, 72, 29-39.

Courtin-Nomade, A., Waltzing, T., Evrard, C., Soubrand, M., Lenain, J.-F., Ducloux, E., Ghorbel, S., Grosbois, C., and Bril, H. (2016) Arsenic and lead mobility: From tailings materials to the aqueous compartment. Applied Geochemistry, 64, 10-21.

Craw, D., Wilson, N., and Ashley, P.M. (2004) Geochemical controls on the environmental mobility of Sb and As at mesothermal antimony and gold deposits. Applied Earth Science, 113, 3-10.

D'Angeli, I.M., Carbone, C., Nagostinis, M., Parise, M., Vattano, M. Madonia, G., and De Waele, J. (2018) New insights on secondary minerals from Italian sulfuric acid caves. International Journal of Speleology, 47, 271-291.

Dutrizac, J.E., and Jambor, J.L. (1987) The behaviour of arsenic during jarosite precipitation: Arsenic precipitation at 97°C from sulphate or chloride media. Canadian Metallurgical Quarterly, 26, 91-101.

Dutrizac, J.E., and Jambor, J.L. (2000) Jarosites and their application in hydrometallurgy. In Alpers, C.N., Jambor, J.L. & Nordstrom, D.K. (eds.) Sulfate Minerals. Crystallography, Geochemistry and Environmental Significance. Reviews in Mineralogy and Geochemistry, 40, pp. 405-452.

Egal, M., Casiot, C., Morin, G., Parmentier, M., Bruneel, O., Lebrun, S., and Elbaz-Poulichet, F. (2009) Kinetic control on the formation of tooeleite, schwertmannite and jarosite by Acidithiobacillus ferrooxidans strains in an As(III)-rich acid mine water. Chemical Geology, 265, 432-441

Feng, R., Wei, C., Tu, S., Ding, Y., Want, R., and Guo, J. (2013) The uptake and detoxification of antimony by plants: A review. Environmental and Experimental Botany, 96, 28-34.

Filippi, M., Drahota, P., Machvič, Böhmová, V., and Mihaljevič, M. (2015) Arsenic mineralogy and mobility in the arsenic-rich historical mine waste dump. Science of the Total Environment, 536, 713-728.

Flores, M., Patiño, F., Palacios, E.G., Reyes, I., Reyes, M., Flores, V.H., Juárez, J.C., and Pandiyan, T. (2016) The behaviour of arsenic during the thermal and chemical decomposition of the ammonium-arsenic jarosite. Preprints, doi:10.20944/preprints201610.0059.v1

Forray, F.L., Smith, A.M.L., Navrotsky, A., Wright, K., Hudson-Edwards, K.A., and Dubbin, W.E. (2014) Synthesis, characterization and thermochemistry of Pb-As-, Pb-Cu- and Pb-Zn-jarosite compounds. Geochimica et Cosmochimica Acta, 127, 107-119.

Foster, A.L., Brown, G.E., Tingle, T.N., and Parks, G.A. (1998) Quantitative arsenic speciation in mine tailings using X-ray absorption spectroscopy. American Mineralogist, 83, 553-568.

Gale, J.D., Wright, K. & Hudson-Edwards, K.A. (2010) A first principles determination of the orientation of H_3O^+ in hydronium alunite. American Mineralogist, 95, 1109-1112.

444 Gieré, R., Sidenko, N.V., and Lazareva, E.V. (2003) The role of secondary minerals in controlling the migration
445 of arsenic and metals from high-sulfide wastes (Berikul gold mine, Siberia). Applied Geochemistry, 18,
446 1347-1359.
447 Gräfe, M., Beattie, D.A., Smith, E., Skinner, W.M., and Singh, B. (2008) Copper and arsenate co-sorption at the
448 mineral-water interfaces of goethite and jarosite. Journal of Colloid and Interface Science, 322, 399-413.
449 Hawthorne, F.C., Krivovichev, S.V., and Burns, P.C. (2000) The crystal chemistry of sulfate minerals. In Alpers,
450 C.N., Jambor, J.L. & Nordstrom, D.K. (eds.) Sulfate Minerals. Crystallography, Geochemistry and
451 Environmental Significance. Reviews in Mineralogy and Geochemistry, 40, pp. 1-112.
452 Henao, D.M.O., and Godoy, M.A.M. (2010) Jarosite pseudomorph formation from arsenopyrite oxidation using
453 Acidithiobacillus ferroxidans. Hydrometallurgy, 104, 162-168.
454 Hudson-Edwards, K.A., Schell, C. and Macklin, M.G. (1999) Mineralogy and geochemistry of alluvium
455 contaminated by metal mining in the Rio Tinto area, southwest Spain. Applied Geochemistry, 14, 1015-1030.
456 Hudson-Edwards, K.A., Jamieson, H.E., Charnock, J.M., and Macklin, M.G. (2005) Arsenic speciation in waters
457 and sediment of ephemeral floodplain pools, Ríos Agrio-Guadiamar, Aznalcóllar, Spain. Chemical Geology,
458 219, 175-192.
459 Jambor, J.L. (1999) Nomenclature of the alunite supergroup. Canadian Mineralogist, 37, 1323-1341.
460 Jambor, J.L., Owens, A.R., Grice, J.D., and Feinglos, M.N. (1996) Gallobeudantite, $PbGa_3[(AsO_4),(SO_4)]_2(OH)_6$,
461 a new mineral species from Tsumbe, Namibia, and associated new gallium analogues of the alunite-jarosite
462 family. Canadian Mineralogist, 34, 1305-1315.
463 Jamieson, H.E., Robinson, C., Alpers, C.N., Nordstrom, D.K., Poustovetov, A., and Lowers, H.A. (2005) The
464 composition of coexisting jarosite-group minerals and water from the Richmond mine, Iron Mountain,
465 California. Canadian Mineralogist 43, 1225-1242.
466 Johnston, S.G., Burton, E.D., Keene, A.F., Planer-Friedrich, B., Voegelin, A., Blackford, M.G., and Lumpkin,
467 G.R. (2012) Arsenic mobilization and iron transformations during sulfidization of As(V)-bearing jarosite.
468 Chemical Geology 334, 9-24.
469 Karimian, N., Johnston, S.G., and Burton, E.D. (2017) Antimony and arsenic behavior during Fe(II)-induced
470 transformation of jarosite. Environmental Science & Technology, 51, 4259-4268.

Karimian, N., Johnston, S.G., and Burton, E.D. (2018) Antimony and arsenic partitioning during Fe^{2+}-induced transformation of jarosite under acidic conditions. Chemosphere, 195, 515-523.

Kendall, M.R., Madden, A.S., Elwood Madden, M.E., and Hu, Q. (2013) Effects of arsenic incorporation on jarosite dissolution rates and reaction products. Geochimica et Cosmochimica Acta, 112, 192-207.

Kolitsch, U., Slade, P.G., Tiekink, E.R.T., and Pring, A. (1999) The structure of antimonian dussertite and the role of antimony in oxysalt minerals. Mineralogical Magazine, 63, 17-26.

Kocourková, E., Sracke, O., Houzar, S., Cempírek, J., Losos, Z., Filip, J., and Hršelová (2011) Geochemical and mineralogical control on the mobility of arsenic in a waste rock pile at Dlouhá Ves, Czech Republic. Journal of Geochemical Exploration, 110, 61-73.

Kubisz J. (1964) A study of minerals in the alunite–jarosite group. Polska Akademia Nauk-Prace Museum Ziemi, 22, 1–93.

Kubisz J. (1970) Studies on synthetic alkali-hydronium jarosites: I. Synthesis of jarosite and natrojarosite. Mineralobia Polonica, 1, 47–57.

Leuz, A.-K., Mönch, H., and Johnson, C.A. (2006) Sorption of Sb(III) and Sb(V) to goethite: influence on Sb(III) oxidation and mobilization. Environmental Science & Technology, 40, 7277-7282.

Luo, Z.Q., Zhou, X.T., Jia, Q.M., Chen, X.F., Tao, Z.CH., and Liu, S.Q. (2015) Preparation of arsenical-natroalunite solid solutions with high crystallinity by hydrothermal method. Materials Research Innovations, 19, No. Sup. 6, S6-S26.

Mitsunobu, S., Muramatsu, C., Watanabe, K., and Sakata, M. (2013) Behavior of antimony (V) during the transformation of ferrihydrite and its environmental implications. Environmental Science and Technology, 47, 9660-9667.

Mitsunobu, S., Takahashi, Y., Terada, Y., and Skata, M. (2010) Antimony(V) incorporation into synthetic ferrihydrite, goethite and natural iron oxyhydroxides. Environmental Science & Technology, 44, 3712-3718.

Nieto, J.M., Capitn, M.A., Sez, R., and Almodóvar, G.R. (2003) Beudantite: A natural sink for As and Pb in sulphide oxidation processes. Applied Earth Science B, 112, 293-296.

Nordstrom, D.K. (1982) The effect of sulfate on aluminum concentrations in natural waters: some stability relations in the system Al_2O_3-SO_2-H_2O at 298 K. Geochimica et Cosmochimica Acta, 46, 681-692.

Paktunc, D., and Dutrizac, J.E. (2003) Characterization of arsenate-for-sulfate substitution in synthetic jarosite using X-ray diffraction and X-ray absorption spectroscopy. Canadian Mineralogist, 41, 905-919.

Paktunc, D., Foster, A., and Laflamme, G. (2003) Speciation and characterization of arsenic in Ketza River mine tailings using X-ray absorption spectroscopy. Environmental Science & Technology, 37, 2067-2074.

Patiño, F., Flores, M.U., Reyes, I.A., Reyes, M., Hernández, J., Rivera, I., and Juárez, J. (2013) Alkaline decomposition of synthetic jarosite with arsenic. Geochemical Transactions, 14:2.

Roca, A., Viñals, J., Arranz, M., and Calero, J. (1999) Characterization and alkaline decomposition/ cyanidation of beudantite-jarosite materials from Rio Tinto gossan ores. Canadian Metallurgical Quarterly, 38, 93-103.

Roussel, C., Néel, C., and Bril, H. (2000) Minerals controlling arsenic and lead solubility in an abandoned gold mine tailings. Science of the Total Environment, 263, 209-219.

Sànchez, L., Cruells, M., Roca, A. (1996) Sulfidization-cyanidation of jarosite species: applicability to the ogssan ores of Rio Tinto. Hydrometallurgy, 42, 35-49.

Savage, K.S., Bird, D.K., and Ashley, R.P. (2000) Legacy of the California Gold Rush: Environmental geochemistry of arsenic in the southern Mother Lode Gold Disctrict. International Geology Review, 42, 385-415.

Savage, K.S., Bird, D.K., and O-Day, P.A. (2005) Arsenic speciation in synthetic jarosite. Chemical Geology, 215, 473-498.

Smeaton, C.M., Walshe, G.E., Smith, A.M.L., Hudson-Edwards, K.A., Dubbin, W.E., Wright, K., Beale, A.M., Fryer, B.J., and Weisener, C.G. (2012) Simultaneous reduction of Fe and As during the reductive dissolution of Pb-As jarosite by *Shewanella putrefaciens* CN32. Environmental Science & Technology, 46, 12823-12831.

Smith, A.M.L., Dubbin, W.E., Wright, K., and Hudson-Edwards, K.A. (2006) Dissolution of lead- and lead-arsenic jarosites at pH 2 and 8: insights from batch experiments. Chemical Geology, 229, 344-361.

Sundar, S., and Chakravarty, J. (2010) Antimony toxicity. International Journal of Environmental Research and Public Health, 7, 4267-4277.

Sunyer, A., and Viñals, J. (2011a) Arsenate substitution in natroalunite: A potential medium for arsenic immobilization. Part 1: Synthesis and compositions. Hydrometallurgy, 109, 54-64.

525 Sunyer, A., and Viñals, J. (2011b) Arsenate substitution in natroalunite: A potential medium for arsenic
526 immobilization. Part 2: Cell parameters and stability tests. Hydrometallurgy 109, 106-115.
527 Sunyer, A., Currubí, M., and Viñals, J. (2013) Arsenic immobilization as alunite-type phases: The arsenate
528 substitution in alunite and hydronium alunite. Journal of Hazardous Materials, 261, 559-569.
529 Szymanski, J.T. (1988) The crystal structure of beudantite, $Pb(Fe,Al)_3[(As,S)O_4](OH)_6$. Canadian Mineralogist,
530 26, 923-932.
531 Viñals, J., Sunyer, A., Molera, P., Cruells, M., and Llorca, N. (2010) Arsenic stabilization of calcium arsenate
532 waste by hydrothermal precipitation of arsenical natroalunite. Hydrometallurgy, 104, 247-259.
533 Welch, S.A., Christy, A.G., Kirste, D., Beavis, S.G. & Beavis, F. (2007) Jarosite dissoluteion I - Trace cation
534 flux in acid sulfate soils. Chemical Geology, 245, 183-197.
535 WHO (World Health Organization) (1996) Health criteria and other supporting information. Pp. 940-949 in:
536 Guidelines for Drinking-water Quality, 2nd edition, Vol. 2. WHO, Geneva.
537 WHO (World Health Organization) (1998) Addendum to Vol. 2. Pp. 281ÿ283 in: Guidelines for drinking- water
538 quality, 2nd edition. WHO, Geneva.
539 Xu, Z., Lǔ, B., Wu, J., Zhou, L., and Lan, Y. (2013) Reduction of Cr(VI) facilitated by biogenetic jarosite and
540 analysis of its influencing factors with response surface methodology. Materials Science and Engineering C,
541 33, 3723-3729.
542 Zheng, M.X., Xu, J.M., Smith, L., and Naidu, R. (2003) Why a fern (Pteris multifida) dominantly growing on an
543 arsenic/heavy metal contaminated soil does not accumulate arsenic. Journal de Physique IV, 107, 1409-1411.
544